Stress reduction and bond stability during thermal annealing of tetrahedral amorphous carbon

A. C. Ferrari,[a] B. Kleinsorge, N. A. Morrison, and A. Hart
Department of Engineering, University of Cambridge, Cambridge, CB2 1PZ, United Kingdom

V. Stolojan
Cavendish Laboratories, University of Cambridge, Cambridge, CB3 OHE, United Kingdom

J. Robertson
Department of Engineering, University of Cambridge, Cambridge, CB2 1PZ, United Kingdom

(Received 16 October 1998; accepted for publication 15 February 1999)

A comprehensive study of the stress release and structural changes caused by postdeposition thermal annealing of tetrahedral amorphous carbon (ta-C) on Si has been carried out. Complete stress relief occurs at 600–700 °C and is accompanied by minimal structural modifications, as indicated by electron energy loss spectroscopy, Raman spectroscopy, and optical gap measurements. Further annealing in vacuum converts sp^3 sites to sp^2 with a drastic change occurring after 1100 °C. The field emitting behavior is substantially retained up to the complete stress relief, confirming that ta-C is a robust emitting material. © *1999 American Institute of Physics.* [S0021-8979(99)05910-1]

I. INTRODUCTION

Three issues have restricted the use of diamond-like carbon (DLC) films as wear-resistive mechanical coatings: their thermal stability, their high compressive stress, and their low toughness.[1–4] DLC is a form of amorphous carbon (*a*-C) or hydrogenated amorphous carbon (*a*-C:H) with a significant fraction of sp^3 bonding. Most DLCs contain hydrogen, and the evolution of this hydrogen, often at relatively low temperatures of 350–400 °C, leads to a loss of sp^3 bonding and a loss of diamond-like properties.[5] There has been considerable work on a hydrogen-free, high sp^3 bonded form of DLC known as tetrahedral amorphous carbon (ta-C). This can be deposited by various methods such as mass selected ion beams,[6] pulsed laser deposition (PLD),[7] magnetron sputtering with ion plating[8] or, as here, filtered cathodic vacuum arc (FCVA).[9,10] This ta-C has a much better thermal stability than *a*-C:H, largely because it does not contain hydrogen.[9–15] In addition, the mechanical properties of ta-C [Young's modulus ~800 GPa, hardness ~70 GPa (Refs. 14, and 16–19)] are much superior to those of most *a*-C:H's, because of its higher C–C coordination.[20]

A second problem with DLCs and particularly ta-C is that the films possess a large intrinsic compressive stress.[10,17] This stress can reach over 10 GPa. It seriously limits the maximum thickness of adherent films that can be deposited, and this inhibits their use as protective coatings, particularly for ta-C. The stress is an intrinsic property of DLC films because it arises from the deposition mechanism known as subplantation, which creates the sp^3 bonding.[6,21–23]

There have been a number of strategies to reduce the stress in as-deposited *a*-C:H films, such as incorporating metals,[24] silicon,[25] or multilayers.[26] However, metal incorporation has drawbacks such as removing the optical transparency of the film. Recently, Friedmann *et al.*[14,27,28] found that postdeposition annealing of PLD ta-C to ~600 °C provides a complete relief of stress, while retaining its diamond-like properties. This allows much thicker (~1 μm) coatings of ta-C to be made by cyclic deposition and annealing, and so provides a means to utilize its outstanding properties.

This article describes a thorough structural investigation of the effect of thermal annealing on ta-C and how its bonding properties are retained, using a variety of measurement techniques such as electron energy loss spectroscopy (EELS), visible Raman, ultraviolet (UV) Raman, optical absorption, and resistivity. Scanning electron microscopy (SEM) was also used in order to investigate some of the morphological changes which accompany the annealing of the film at very high temperatures (>1100 °C).

The fraction of sp^3 bonding in ta-C depends on the ion energy used in deposition and it reaches a maximum of about 85% for an ion energy of about 100 eV. Most of the properties of as-deposited ta-C such as density, optical gap, elastic modulus, hardness, and stress correlate directly with the sp^3 content.[10]

II. EXPERIMENT

The FCVA used to deposit the ta-C films is described elsewhere.[10] Two series of ta-C samples were deposited by FCVA at room temperature at a mean ion energy of 100 eV and a deposition rate of about 0.7 nm/s. This maximizes the sp^3 content and the stress in ta-C films. One series was deposited on heavily doped *n*-type Si(100) for the stress, EELS, Raman and field emission measurements, and the second series on quartz for optical gap and resistivity measurements, with thickness around 70 and 30 nm, respectively.

The sp^3 content and the mass density were obtained from the carbon *K*-edge EELS and from the plasmon energy in the low energy EELS spectrum, as described previously.[10] The EELS measurements were carried out on a dedicated

[a]Electronic mail: acf26@eng.cam.ac.uk

100 kV VG 501 scanning transmission electron microscope, fitted with a spectrometer with a McMullan parallel EELS detection system.[29] The plasmon energies were fitted by the plasmon loss function of a free electron gas.[30] The film thicknesses were determined by surface profilometer measurements (Sloan DektaK II) and also by ellipsometry (Gaertner Scientific L117). The optical gap (E_{04} and Tauc) and complex refractive index were measured using an Ati-UNICAM UV-visible spectrometer. Resistivity measurements were carried out in the coplanar configuration using single gap cells. Before annealing, each sample on quartz was divided in two parts: One of them was annealed at the chosen temperature and then aluminum contacts were thermally evaporated on both of them. A Hewlett Packard 4140B picoampere meter was used for the measurements.

Unpolarized visible Raman spectra were recorded in backscattering geometry for 514.5 nm excitation from an Ar ion laser using a Jobin–Yvon T64000 triple grating spectrometer or a SPEX 1401 double monochromator, both in the microconfiguration. The spectral resolution was 3–6 cm^{-1}. The UV Raman spectra were collected on an UV-enhanced charge coupled device camera on a Renishaw micro-Raman System 1000 spectrometer modified for use at 244 nm with fused silica optics throughout with a spectral resolution of 3 cm^{-1}. The UV-Raman spectra used the 244 nm line of an intracavity frequency-doubled Ar laser (Coherent Innova 300 series). During each Raman experiment, a laser output of 10 mW was used, resulting in 1 mW on a spot of ~ 1 μm^2. Under these conditions no sample damage was observed. The Raman samples were obtained by breaking a single large sample.

The field emission measurements were carried out in the parallel plate configuration with an anode of indium tin oxide coated glass, a plate spacing of 50 μm defined by Makor spacers, and in a chamber maintained by liquid N_2-trapped diffusion pump at under 5×10^{-7} Torr.[31]

A first series of annealing experiments was carried out in an unsealed tube furnace swept by flowing dry nitrogen. Each sample was heated for 5 min incremental periods up to 60 min, at a predetermined annealing temperature. After each period, the sample was cooled in air and the stress was derived by Stoney's equation[32] from the substrate curvature measured by a surface profilometer. No film delamination occurred. No appreciable change in the bare Si substrate curvature was detected following annealing. The thickness was found to dramatically decrease at temperatures above 400 °C due to oxidation.

To reach higher temperatures, further annealing experiments were carried out under vacuum, between 10^{-7} and 10^{-5} mbar, both by the use of a heated sample holder (up to 1000 °C) and by resistive heating of the substrate (higher temperatures). The heating cycle consisted of a ramp of $\sim$40 min (with the heated plate) or 2 min (while resistively heating the substrate). The preselected temperature was then maintained for 20 min. The samples were then allowed to cool fully for 40 min before opening to air, to avoid oxidation. A 20 min anneal time was chosen for these experiments being the shortest safe time to the steady state stress value, as shown by the time resolved stress release in the furnace (Fig. 1). Following vacuum heat treatment, the films were characterized in terms of their intrinsic stress, Raman spectra, optical gap, resistivity, and field emission properties as described earlier. Delamination was observed for samples on Si only for temperatures higher than 1100 °C

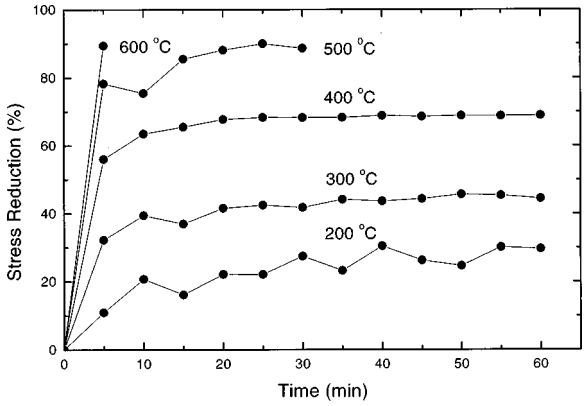

FIG. 1. Stress reduction as a function of annealing time for samples annealed in a nitrogen furnace at various temperatures.

III. RESULTS

The stress of the as-deposited ta-C films (at a mean ion energy of 100 eV) was 11 GPa. Figure 1 plots the fractional stress reduction against annealing time for the samples annealed in nitrogen. Figure 2 shows the steady state stress reduction as a fraction of the original stress for films annealed in nitrogen or vacuum. These results suggest that a universal stress relief process occurs irrespective of the environment, as proposed by Sullivan *et al.*,[27,28] who found the same behavior for PLD ta-C deposited on Si, TiW coated Si, and sapphire.

Figure 3 shows the sp^3 fraction of the films from EELS as a function of the anneal temperature. The sp^3 fraction starts at 87% and remains constant up to $\sim$700 °C, within the accuracy of the measurement. Subsequently it decreases slightly up to 1100 °C and then it falls to less than 20%. These data show that the sp^3 bonding of ta-C is retained above the stress relief temperature of 600 °C, extending the data of Friedmann[13,14] and Anders[11,12] on thermal stability.

Figure 4 shows the plasmon energy of the films versus

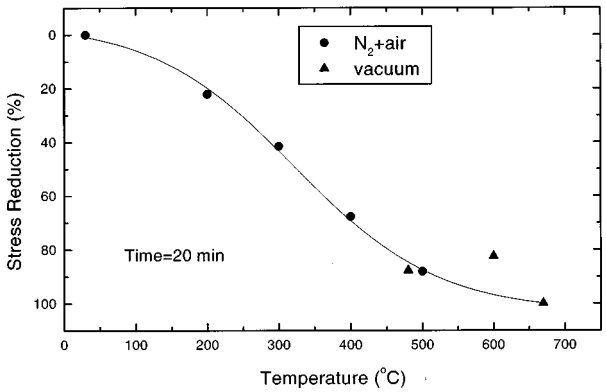

FIG. 2. Steady state stress reduction as a function of annealing temperature, for samples annealed both in flowing nitrogen and in vacuum.

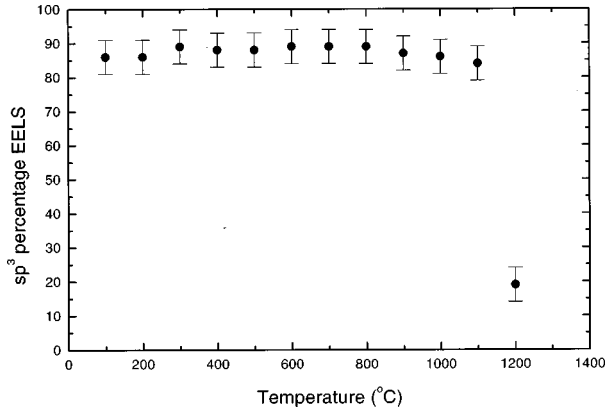

FIG. 3. sp^3 fraction as a function of annealing temperature.

annealing temperature. The plasmon energy is a measure of the density. It starts at 32 eV, corresponding to a density of 3.1 $g\,cm^{-3}$, it remains roughly constant to about 1100 °C, and then declines. This measurement supports the sp^3 data as the sp^3 fraction and density are usually strongly correlated. Our plasmon energy plot, together with others,[14,15] do not show the density reduction seen in some x-ray reflectivity measurements.[33]

Sullivan *et al.*[27,28] proposed a structural model for stress relief, discussed in more detail later, in which a small fraction of sp^3 sites convert to sp^2 to relieve stress. sp^2 sites control the band gap[34] and the new sp^2 sites could decrease the band gap, or introduce states in the gap which increase the subgap absorption and the conductivity.

Figure 5(a) shows the optical gap derived from optical absorption and reflectivity measurements. Transmission and reflection spectra were taken using an Ati-UNICAM UV-visible spectrometer. Formulae for multiple reflection and transmission in thin films were used to find the complex refractive index of the samples.[35] As thickness and an approximate value of the real part of the refractive index are known, this method gives good results for the imaginary part of the refractive index from which the absorption coefficient can be derived. This method does not depend on diffraction fringes. The optical gap remains at about 2.67 eV up to 670 °C. It then declines to under 1 eV at 900 °C.

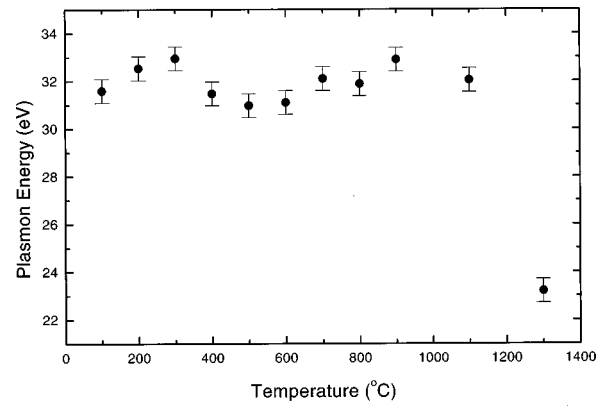

FIG. 4. Plasmon energy as a function of annealing temperature.

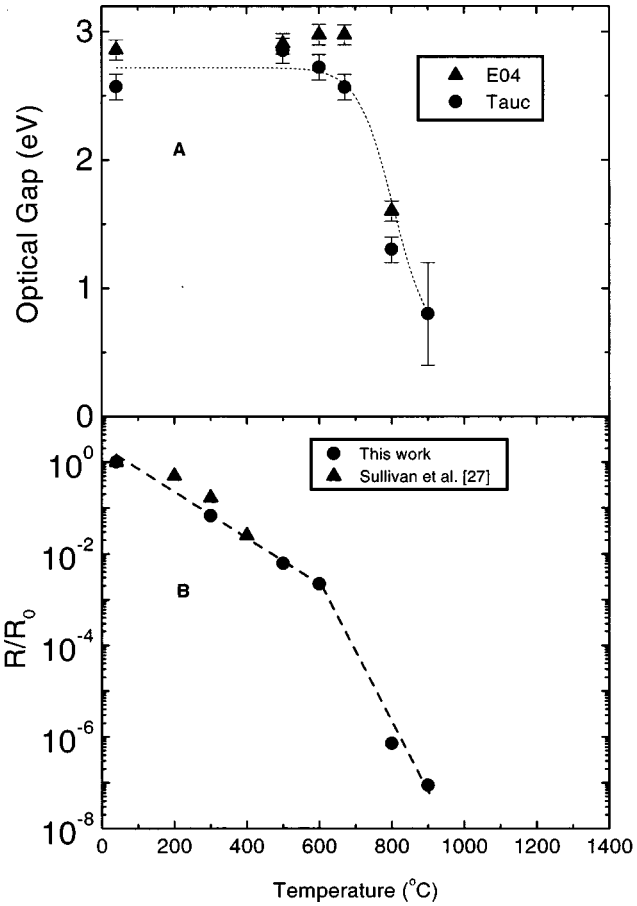

FIG. 5. (a) Variation of optical gap (Tauc, E_{04}) vs annealing temperature; the line is a guide to the eye. No experimental data are available at T higher than 900 °C due to delamination from quartz, but the higher sp^2 content is expected to reduce the gap (Ref. 34). E_{04} is higher than Tauc gap in ta-C (and in DLC in general) (Refs. 34 and 53). (b) Variation of resistivity with annealing temperature. R/R_0 denotes the ratio of resistivity after annealing and before annealing. ●, this work, ▲ Sullivan, Friedmann, and Baca (Ref. 27). The line is a guide to the eye.

Figure 5(b) shows the decrease in resistivity with annealing comparing our data on FCVA ta-C with the ones of Sullivan, Friedmann, and Baca[27] on PLD ta-C. The resistivity of a typical as-deposited film is $\sim 10^7\ \Omega\,cm$. The resistivity shows a slow exponential fall up to 600 °C, followed by a sharper drop at higher temperatures. The correlation between gap and resistivity will be assessed in more detail later.

A deeper understanding of the bonding changes is possible from Raman spectroscopy.[23] It is well known that visible Raman at 514 nm is directly sensitive only to the sp^2 sites in carbon, because this photon energy preferentially excites the π states on the sp^2 sites. This is reflected in the roughly 55 times higher cross section of graphite than bulk diamond[36] and a possible ~233 times higher cross section of amorphous carbon than diamond.[37] Recently, UV Raman at 244 nm has been introduced.[38,39] Its higher photon energy of 5.1 eV can excite both the π and σ states, and so is able to probe both the sp^2 and sp^3 sites with a similar cross section. This now allows a direct probe of sp^3 bonding.

Figure 6 shows the UV Raman spectra of an as-deposited film and after various anneal temperatures. The

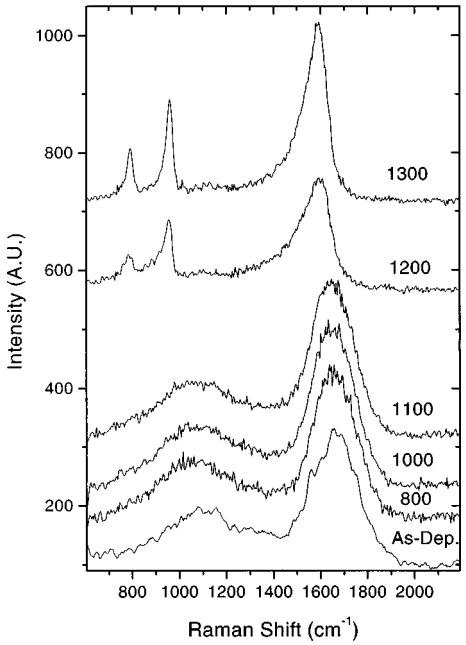

FIG. 6. UV (224 nm) Raman spectra of as-deposited ta-C and samples annealed to the indicated temperatures; the peaks at 792 and 955 cm^{-1} in the 1200 and 1300 °C are signatures of SiC (Refs. 45 and 46). Si substrate does not give any signal in UV Raman, due to its high UV absorption.

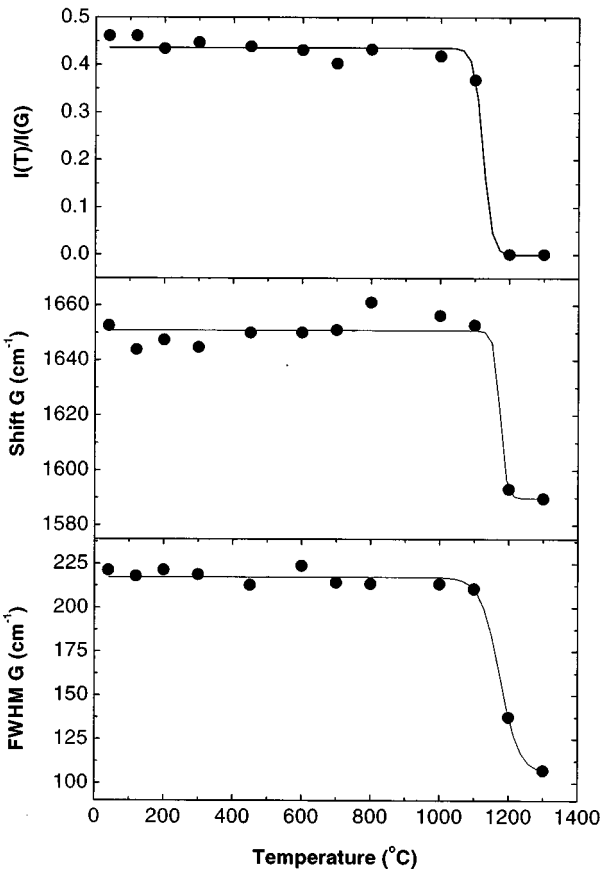

FIG. 7. Variation of $I(T)/I(G)$ ratio, G peak position and G peak FWHM of the UV Raman spectra of Fig. 6 vs annealing temperature; the liens are guide to the eye.

spectra consist of two main features, a ''G'' peak at 1660 cm^{-1} attributed to bond stretching vibrations of C═C groups, and a ''T'' peak at about 1050 cm^{-1} attributed to all sp^3 C–C bond vibrations.[38] The intensity ratio of the T and G peaks, $I(T)/I(G)$, of as-deposited ta-C films is found to correlate strongly with their sp^3 fraction.[38–40] It is also found that the position and width of the G peak correlate with the sp^3 fraction.

Figure 7 shows the variation of the $I(T)/I(G)$ ratio, G peak position and full width at half maximum (FWHM) in UV Raman as a function of annealing temperature. All three values are seen to remain roughly constant to at least 1000 °C. This shows that the overall sp^3 bonding of ta-C is maintained to 1100 °C, in agreement with the EELS data of Figs. 3 and 4.

Figure 8 shows the visible Raman spectrum of ta-C, as deposited and after various anneal temperatures. The spectrum of as-deposited ta-C displays one main feature, a broad G peak at 1567 cm^{-1} without any sign of D peak. The G peak in ta-C can be fitted with a skewed Lorentzian or Breit–Wigner–Fano (BWF) function.[41] In Fig. 9, the G band position is given as the maximum of the BWF rather than its center, to allow a comparison with literature data using a symmetric line shape fitting. For annealed films above 600 °C, a second D Lorentzian peak is needed to fit the spectrum properly. The D peak is attributed to the zone boundary mode of graphitic clusters and is not present in as-deposited FCVA ta-C films. In microcrystalline graphite, the ratio $I(D)I(G)$ of the D and G peaks correlates inversely with the grain size, but the opposite relationship applies for amorphous carbons, where the grains are under 2 nm in diameter:[42,43] Generally, a D peak is an indication that the sp^2 sites are organizing into graphitic rings.[36,42–44]

Figure 9 shows the intensity ratio of the D and G peaks, $I(D)/I(G)$, the position, and FWHM of the G peak as a function of the annealing temperature. All three values move towards values characteristic of sp^2 bonding.[41,44] This occurs earlier and more gradually than the features in UV Raman. Thus the change towards more sp^2 bonding is seen in visible Raman before they become apparent in UV Raman. This is consistent with the much greater sensitivity of visible Raman to sp^2 bonding. These data confirm the decrease in sp^3 fraction (a few percent more than the 5% resolution) detected by EELS for films annealed above 800 °C.

SEM indicates that surface morphology changes abruptly between 1100 and 1200 °C passing from a very smooth structureless surface to a rough, pitted one showing ~ 2 μm sized features. These are β-SiC grains formed by a reaction of the carbon film with the Si substrate, as indicated by the transverse optical and longitudinal optical phonons at 792 and 955 cm^{-1} detected by micro-Raman spectroscopy (both visible and UV, Fig. 6)[45,46] and by the observation of the Si-*L* edge at 100 eV in EELS. Note that Si substrate gives no signal in the UV Raman spectrum, due to its high UV absorption ($\sim 3\times 10^6$ cm^{-1}). The SiC formation process is favored by the high mobility of the Si surface atoms at such temperature. While the SiC Raman peaks are visible only inside these grains, the spectra in Figs. 6 and 8 for the samples annealed at 1200 and 1300 °C do not show signifi-

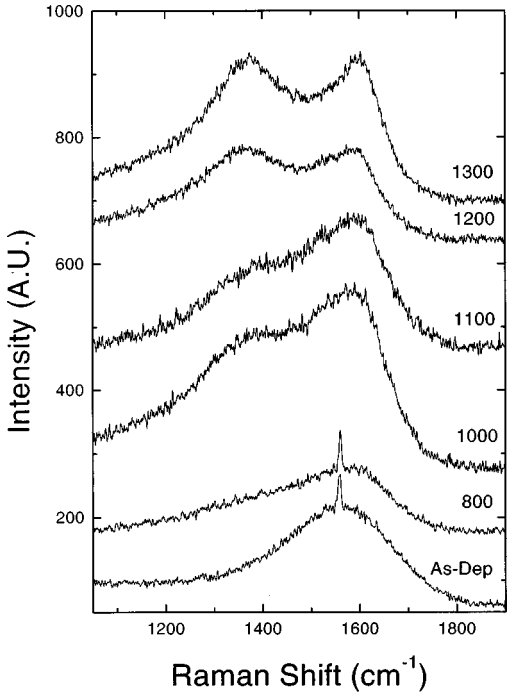

FIG. 8. Visible (514 nm) Raman spectra of as-deposited ta-C and some samples annealed to the indicated temperatures; the sharp peak at 1555 cm^{-1} in the as-deposited and 800 °C spectra is due to atmospheric O_2. It is not visible for samples annealed at higher temperature due to the higher intensity of the carbon Raman peaks. The intensity of Si substrate peaks (not shown) decreases with annealing T (Ref. 13).

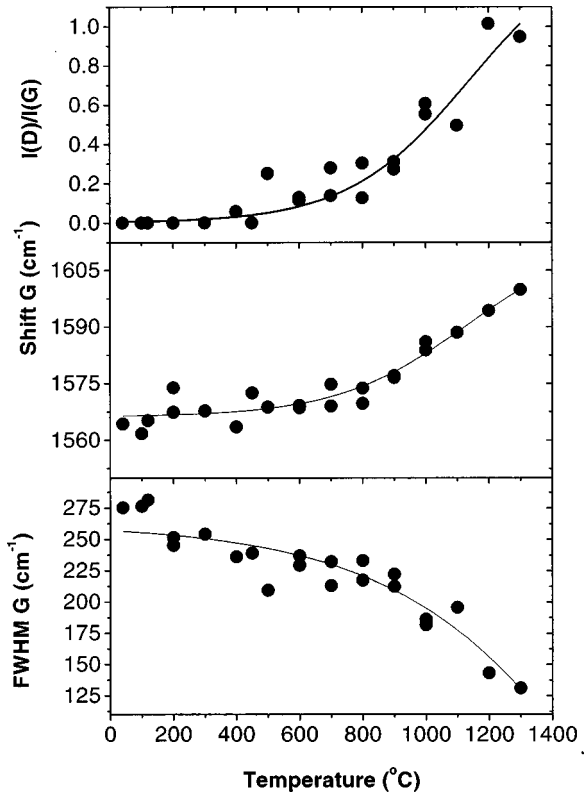

FIG. 9. Variation of G peak position, $I(D)/I(G)$ ratio and G peak position and G peak FWHM of the visible Raman spectra of Fig. 8, vs annealing temperature; the lines are guide to the eye.

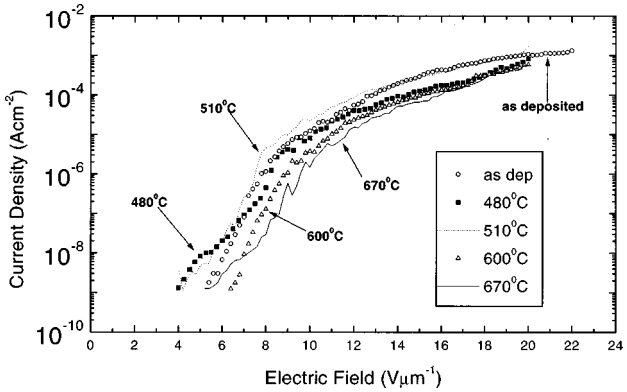

FIG. 10. J–E plots for as-deposited and annealed samples. The threshold field is defined as the field corresponding to an emission of 1 $\mu A/cm^2$ (Ref. 31). It is between 7.5 and 9.7 V/μm in all the samples.

cant changes outside the grains in the frequency region with the amorphous carbon signature.

Figure 10 shows the field emission current density versus electric field for the as-deposited films and after annealing to 480, 510, 600, and 670 °C. There is little change in the overall J–E plots, confirming that the surface properties of ta-C are also remarkably resilient to annealing. Investigations of the field emission behavior at higher temperatures in order to relate the sp^2 clustering with the emitting threshold is in progress and will be reported elsewhere.

IV. DISCUSSION

The optical, EELS, and Raman data clearly indicate that complete stress relief in ta-C may be achieved by annealing under vacuum at 600–670 °C after deposition, without major changes in bonding. This is shown by the constancy of the optical gap and the Raman spectra. This bond stability has already been observed by EELS and near edge x-ray absorption fine structure[11,14,15] but it has been confirmed here by the simple nondestructive method of UV Raman. The substantial stability of the G wave number and its width in both the UV and the visible Raman confirm the only very slight changes in the film structure. In Fig. 9, a change in the visible Raman parameters and, in particular, an increase of $I(D)/I(G)$ occurs from around 700 °C. The increase in the D peak is an indication of the state of development of the sp^2 phase and that the sp^2 sites are beginning to organize into small graphitic clusters.

Sullivan *et al.*[27,28] noted that while the atomic volume of sp^2 site exceeds that of a sp^3 site, its in-plane size is less, due to its shorter bond length. Thus, the formation of sp^2 sites with their σ plane aligned in the plane of compression will relieve a biaxial compressive stress. The changes in stress and strain in a thin film under biaxial stress are related by[32]

$$\Delta\sigma = \frac{E}{1-\nu}\Delta\epsilon, \tag{1}$$

where σ is the stress, E the Young's Modulus, ν the Poission's ratio, and ϵ is the strain. We have neglected any variations in elastic constants and attributed all the stress relief to

strain variation. Taking the change in film stress as $\Delta\sigma \sim 10$ GPa and $E/(1-\nu) \sim 1000$ GPa (Refs. 18 and 19) the strain variation $\Delta\epsilon$ is found to be $\sim 1\%$. Thus only a small change in the strain is needed to give the observed stress release. This can be accounted for by a slight decrease in the density, not detectable within the error of EELS. If we attribute the strain variation to decrease in sp^3 fraction, the fraction of sp^2 sites needed is $\Delta n \sim 1\%$. Thus only a small increase in sp^2 fraction is needed to account for the stress relief.

Figure 9 shows the onset of sp^3 to sp^2 conversion at ~ 700 °C, as indicated by the knee in the visible Raman data. On the other hand the UV Raman data shown in Fig. 7 remain virtually constant until ~ 1100 °C, when an abrupt transition is observed and $I(T)/I(G)$, the G band frequency and its FWHM all decrease. This contrasts with the smoother transition of the parameters of visible Raman.

The optical gap stays constant until 670 °C, then begins to decrease. The Tauc gap at 900 °C is less than 1 eV compared to 2.67 eV of the as-deposited samples and it is expected to decrease further as the sp^2 content increases.[34] The resistivity decreases exponentially with the annealing temperature much earlier than any changes become clearly apparent in EELS, visible Raman or in optical gap and it drops quickly after 600 °C. McCulloch *et al.*[51] also reported substantial changes in resistivity not paralleled by changes in optical gap and sp^3 fraction in ion implanted ta-C.

In summary: UV Raman is least sensitive to the appearance of a small fraction of sp^2 sites; visible Raman and optical gap are intermediate and are more sensitive to the clustering of the newly formed sp^2 sites; resistivity is most sensitive to the presence of new sp^2 sites (even if they are not clustering).

It should be noted that the position of the G peak in visible Raman never decreases. Typical Raman spectra obtained from as-deposited sp^2 *a*-C have a G peak at 1520–1540 cm^{-1}.[12] This contrasts with the annealed ta-C, although the annealing eventually forms a graphitic film. This implies that an as-deposited *a*-C has a different structure when compared to a film with similar low sp^3 content following the high temperature annealing of ta-C. This means that, whenever sixfold rings form in the annealed ta-C, they are already well ordered compared to the sp^2 sites of an as-deposited *a*-C.

Our results allow three important clarifications of the Raman spectra in amorphous carbons. First, in our opinion they show that the high frequency of the G peak in ta-C is not due to its high compressive macroscopic stress as has been suggested,[42,47] as the G peak does not decrease when the stress is removed by annealing, as found also by other groups on ta-C made by both FCVA and PLD.[11–14] It should be again pointed out that we verified that annealing up to a complete stress release induces minimal structural changes in ta-C and that also ta-C with very high conductivity and low gap has been reported having high stress.[42]. Second, the G peak in ta-C is blueshifted in both UV Raman (~ 1660 cm^{-1} compared to 1590 cm^{-1} for sp^2 bonded *a*-C) and in visible Raman (~ 1567 cm^{-1} compared to 1540 cm^{-1} or less for sp^2 *a*-C). This is due to the contribution of olefinic sp^2 groups which have shorter C–C bond lengths and higher vibrational frequencies.[38,48–50] Furthermore, the G peak lies higher in UV Raman than in visible Raman because UV Raman is more sensitive to short olefinic groups because 244 nm can excite all the π states, not just the lower energy transitions of more graphitic sp^2 groups.

Third, we showed how a quantitative link between the $I(D)/I(G)$ ratio and the sp^3 content cannot be established in general and that $I(D)/I(G)$ is more sensitive to the clustering of the sp^2 phase, than to the conversion of sp^3 sites in sp^2 ones. The high sensitivity of visible Raman to the ordering of the sp^2 phase would give, e.g., a graphitic spectrum even for a high sp^3 material containing small graphitic microcrystals, as seen for example by McCulloch *et al.*[51] and Schwan *et al.*[42,52]

The structural modification induced by annealing ta-C can therefore be described as follows. Below 600–700 °C only a very small fraction of new sp^2 sites are formed, most probably inside a completely sp^3 phase without any appreciable increase of sp^2 clustering. This causes the exponential increase of the conductivity, due to the increase of hopping centers, while the optical gap and $I(D)/I(G)$ ratio remain constant, being governed by the clustering of the sp^2 sites. A ~ 450 times increase in resistivity, as we detected for ta-C annealed at 600 °C, can be accounted with a $\sim 6\%$ increase in sp^2, according to Sullivan *et al.*[27,28] Thereafter, as the sp^2 content is increased, sp^2 bonded chains begin to cluster into ordering rings, which may either remain isolated or linked together by olefinic chains. This can account for the significant lowering of the optical gap, which does not follow the sp^3 evolution, being governed by the ordering in the sp^2 phase,[34,52,53] and for the drop in resistivity.[51,53] At 1200 °C the number of new sp^2 sites is such that a percolation of the sp^2 islands takes place leading to a graphitic material. This gives rise to a sharp decrease in the UV Raman parameters of Fig. 7, until values approaching those observed in visible Raman are obtained. Further investigations are needed to check if the sp^2 evolution at 1200 °C is triggered by SiC formation or if it is substrate independent.

The high thermal stability of ta-C after deposition contrasts with the much lower transition temperature to sp^2 bonding found during deposition itself, of about 200 °C.[53] This implies that the relaxation process during and after deposition have significant differences. It is often stated that compressive stress is required to stabilize the metastable sp^3 bonding in DLC.[21,52] Clearly, this is not true in general, but only during deposition itself: Once the sp^3 phase is achieved there is no more need of stress for its stabilization and the stress can be released without any appreciable structural change. One should note, however, that the thermal stability is much less for sp^2-rich *a*-C formed at other ion energies, and particularly in nitrogen doped ta-C.[12,13,54]

The relative stability of the field emission current to annealing up to 670 °C, while the resistivity decreases exponentially with the temperature, suggests that field emission depends more on surface or interface properties and on the clustering of newly formed sp^2 sites than on resistivity itself.

V. CONCLUSIONS

It has been demonstrated that the intrinsic compressive stress of ta-C on Si can be completely released with minimal structural changes by a postdeposition anneal to 600–700 °C. No significant variations in the optical gap, EELS, field emission, and UV or visible Raman spectra are observed up to complete stress release. The decrease of electrical resistivity can be accounted for by a slight increase in hopping centers. As there is only a very slight decrease in the sp^3 content, the mechanical properties are expected to exhibit similar thermal stability.[11] Moreover the structure is maintained up to 400 °C when annealed in noninert atmosphere. An abrupt change in the film properties occurs after 1100 °C. We have shown how UV Raman can follow the gross sp^3 changes in the film, while visible Raman provides a powerful way to follow the evolution and the ordering of the sp^2 phase. A simple model to account for the stress relief and for the structural and electrical modifications throughout the annealing was also presented. The release of stress via thermal annealing can be an effective way to grow thick films and to improve the coating properties of ta-C whenever a high temperature treatment is allowed.

ACKNOWLEDGMENTS

The authors would like to thank UK Engineering and Physical Research Council for the financial support. Two of the authors (A. C. F. and B. K.) acknowledge funding by European Community TMR Marie Curie Fellowships. In addition, they would like to thank C. E. Bottani of Politecnico di Milano and D. N. Batchelder of University of Leeds for Raman facilities, B. Breton (CUED) for the SEM pictures and also A. Flewitt, J. Conyers, A. Buckley, and G. Adamopoulos for their help in the data collection.

[1] J. Robertson, Surf. Coat. Technol. **50**, 185 (1992).
[2] A. Matthews and S. S. Eskildsen, Diamond Relat. Mater. **3**, 902 (1994).
[3] A. Grill, Surf. Coat. Technol. **94**, 507 (1997).
[4] M. A. Tamor, Mater. Res. Soc. Symp. Proc. **383**, 423 (1995).
[5] B. Dischler, A. Bubenzer, and P. Koidl, Solid State Commun. **48**, 105 (1983).
[6] Y. Lifshitz, G. D. Lempert, and E. Grossman, Phys. Rev. Lett. **72**, 2753 (1994).
[7] A. Voevodin, M. S. Donley, and J. S. Zabinski, Surf. Coat. Technol. **52**, 42 (1997).
[8] J. Schwan, S. Ulrich, H. Roth, H. Ehrhardt, S. R. P. Silva, J. Robertson, R. Samlenski, and R. Brenn, J. Appl. Phys. **79**, 1416 (1996).
[9] D. R. McKenzie, Rep. Prog. Phys. **59**, 1611 (1996).
[10] P. J. Fallon, V. S. Veerasamy, C. A. Davis, J. Robertson, G. A. J. Amaratunga, and W. I. Milne, Phys. Rev. B **48**, 4777 (1993).
[11] S. Anders, J. Diaz, J. W. Ager, R. Y. Lo, and D. B. Bogy, Appl. Phys. Lett. **71**, 3367 (1997).
[12] S. Anders, J. W. Ager, G. M. Pharr, T. Y. Tsui, and I. G. Brown, Thin Solid Films **308**, 186 (1997).
[13] T. A. Friedmann, K. F. McCarty, J. C. Barbour, M. P. Siegal, and D. C. Dibble, Appl. Phys. Lett. **68**, 1643 (1996).
[14] T. A. Friedmann, J. P. Sullivan, J. A. Knapp, D. R. Tallant, D. M. Follstaedt, D. L. Medlin, and P. B. Mirkarimi, Appl. Phys. Lett. **71**, 3820 (1997).
[15] D. R. McKenzie, Y. Yin, N. A. Marks, C. A. Davis, B. A. Pailthorpe, G. A. J. Amaratunga, and V. S. Veerasamy, Diamond Relat. Mater. **3**, 353 (1994).
[16] G. M. Pharr *et al.*, Appl. Phys. Lett. **68**, 779 (1996).
[17] S. Xu, D. Flynn, B. K. Tay, S. Prawer, K. W. Nugent, S. R. P. Silva, Y. Lifshitz, and W. I. Milne, Philos. Mag. B **76**, 351 (1997).
[18] B. Schultrich, H. J. Scheibe, D. Drescher, and H. Ziegele, Surf. Coat. Technol. **98**, 1097 (1998).
[19] M. G. Beghi, C. E. Bottani, R. Ferulano, P. M. Ossi, R. Pastorelli, L. Giovannini, F. Nizzoli, A. C. Ferrari, and J. Robertson, in *Proceedings of the XVIth International Conference on Raman Spectroscopy*, edited by A. M. Heyns (Wiley, Chichester, 1998), p. 870.
[20] J. Robertson, Phys. Rev. Lett. **68**, 220 (1992).
[21] J. Robertson, Diamond Relat. Mater. **4**, 361 (1993).
[22] C. A. Davis, Thin Solid Films **226**, 30 (1993).
[23] M. A. Tamor and W. C. Vassell, J. Appl. Phys. **76**, 3823 (1994).
[24] H. Dimigen, H. Hubsch, and R. Memming, Appl. Phys. Lett. **50**, 1056 (1987).
[25] K. Okuri and T. Arai, Surf. Coat. Technol. **47**, 710 (1991).
[26] J. Meneve, E. Dekempeneer, W. Wagner, and J. Smeets, Surf. Coat. Technol. **86**, 617 (1996).
[27] J. P. Sullivan, T. A. Friedmann, and A. G. Baca, J. Electron. Mater. **26**, 1021 (1997).
[28] J. P. Sullivan, T. A. Friedmann, R. G. Dunn, E. B. Stechel, P. A. Schultz, M. P. Siegal, and N. Missert, Mater. Res. Soc. Symp. Proc. **498**, 97 (1998).
[29] D. McMullan, P. J. Fallon, J. Ito, and A. J. McGibbon, EUREM 92, Granada, Spain, 1992, p. 103.
[30] R. F. Egerton, *Electron Energy Loss Spectroscopy in the Electron Microscopy* (Plenum, New York, 1986).
[31] B. S. Satyanarayana, A. Hart, W. I. Milne, and J. Robertson, Appl. Phys. Lett. **71**, 1430 (1997).
[32] D. L. Smith, *Thin Film Deposition* (McGraw–Hill, New York, 1995).
[33] L. J. Martinez-Miranda, J. P. Sullivan, T. A. Friedmann, M. P. Siegal, and N. J. DiNardo, Mater. Res. Soc. Symp. Proc. **498**, 55 (1998).
[34] J. Robertson and E. P. O'Reilly, Phys. Rev. B **35**, 2946 (1987).
[35] O. S. Heavens, *Optical Properties of Thin Solid Films*, London, 1955.
[36] N. Wada, P. J. Gaczi, and S. A. Solin, J. Non-Cryst. Solids **35&36**, 543 (1980).
[37] S. R. Salis, D. J. Gardiner, M. Bowden, J. Savage, and D. Rodway, Diamond Relat. Mater. **5**, 589 (1996).
[38] K. W. R. Gilkes, H. S. Sands, D. N. Batchelder, J. Robertson, and W. I. Milne, Appl. Phys. Lett. **70**, 1980 (1997).
[39] V. I. Merkulov, J. S. Lannin, C. H. Munro, S. A. Asher, V. S. Veerasamy, and W. I. Milne, Phys. Rev. Lett. **78**, 4869 (1997).
[40] S. Prawer and K. Nugent, in *Amorphous Carbon: State of the Art*, edited by S. R. P. Silva *et al.* (World Scientific, Singapore, 1998), p. 199.
[41] S. Prawer, K. W. Nugent, Y. Lifshitz, G. D. Lempert, E. Grossman, J. Kulik, I. Avigal, and R. Kalish, Diamond Relat. Mater. **5**, 433 (1996).
[42] J. Schwan, S. Ulrich, V. Bathori, H. Ehrhardt, and S. R. P. Silva, J. Appl. Phys. **80**, 440 (1996).
[43] J. Robertson, Prog. Solid State Chem. **21**, 199 (1991).
[44] R. O. Dillon, J. A. Woollam, and V. Katkanant, Phys. Rev. B **29**, 3482 (1984); M. A. Tamor, J. A. Haire, C. H. Wu, and K. C. Hass, Appl. Phys. Lett. **54**, 123 (1989).
[45] Z. C. Feng, A. J. Mascarenhas, W. J. Choyke, and J. A. Powell, J. Appl. Phys. **64**, 3176 (1998).
[46] D. Olego and M. Cardona, Phys. Rev. B **25**, 1151 (1982).
[47] S. Ager, S. Anders, A. Anders, and I. G. Brown, Appl. Phys. Lett. **66**, 3444 (1995).
[48] D. A. Drabold, P. A. Fedders, and P. Stumm, Phys. Rev. B **49**, 16415 (1994).
[49] T. Kohler, T. Frauenheim, and G. Jungnickel, Phys. Rev. B **52**, 11837 (1995).
[50] G. Herzberg, *Molecular Spectra II: Infrared and Raman Spectra of Polyatomic Molecules* (Van Nostrand, Princeton, 1945).
[51] D. G. McCulloch, E. G. Gerstner, D. R. McKenzie, S. Prawer, and R. Kalish, Phys. Rev. B **52**, 850 (1995).
[52] J. Schwan, S. Ulrich, T. Theel, H. Ehrhardt, P. Becker, and S. R. P. Silva, J. Appl. Phys. **82**, 6024 (1997).
[53] M. Chhowalla, J. Robertson, C. W. Chen, S. R. P. Silva, C. A. Davis, G. A. J. Amaratunga, and W. I. Milne, J. Appl. Phys. **81**, 139 (1997).
[54] S. Bhargava, H. D. Bist, A. V. Narlikar, S. B. Samanta, J. Narayan, and H. B. Tripathi, J. Appl. Phys. **79**, 1917 (1996).